August 27-31, 2023
FLORENCE - ITALY
ICWE 16
16th International Conference on Wind Engineering

Study on stability of vehicles crossing long-span bridge under strong winds

Haeyoung Kim[1], Hiroshi Katsuchi[2], Dionysius M. Siringoringo[3], Yozo Fujino [4], Hitoshi Yamada [5]

[1]*Tokyo University of Science, Tokyo, Japan, kimhy@s.jniosh.johas.go.jp*
[2] *Yokohama National University, Yokohama, Japan, katsuchi@ynu.ac.jp*
[3] *Yokohama National University, Yokohama, Japan, dion@ynu.ac.jp*
[4] *Yokohama National University, Yokohama, Japan, fujino-yozo-bv@ynu.ac.jp*
[5] *Yokohama National University, Yokohama, Japan, yamada-hitoshi-cj@ynu.ac.jp*

SUMMARY:
This paper describes a study on vehicle stability when crossing the bridges of Tokyo Aqua-line Expressway under strong crosswind. CFD was carried out to obtain the aerodynamic coefficients of vehicle on various lane position of bridge deck. Wind forces on the vehicle are computed based on aerodynamics coefficients for various wind speed. Using a 7-degree-of-freedom vehicle model, normal forces on the wheels are quantified. Two vehicle stability conditions were defined: critical rollover and critical rotation. The former is when one of the wheels lose contact force, while the latter is when lateral forces on one axle exceeds the rotation resistance provided by friction between wheel and road pavement. Wind speed limit associated with each critical condition is determined. Results show the windward lane has the smallest wind speed limit and critical rotation occurs earlier than rollover in any lane.

Keywords: vehicle on bridge, vehicle stability, critical wind speed

1. INTRODUCTION

Forty-three vehicle rollover accidents were reported in the Kansai region, Japan by Typhoon *Cimaron* and *Jebi* in 2018. Most accidents were occurred on the strait bridge. The vehicle stability on the bridge under cross wind became more important concerns since it is more susceptible to crosswinds on the strait bridge. Although traffic regulations are taken in strong winds, the criteria for judgment are poor in scientific grounds and the situation of rollover accidents has not been prevented. Many researches have been conducted to calculate the aerodynamic coefficient of vehicles by focusing on a certain bridge by wind tunnel experiments (Zhu, 2012) and numerical fluid analysis (Wang, 2013). However, these studies focus only on the aerodynamic coefficients of vehicles, and there are not so many systematic studies of vehicle instability phenomena such as how it affects the motion of the vehicle. In the Tokyo Bay Aqua Line, two rollover accidents have occurred in the past due to strong winds. To prevent rollover accidents, traffic is restricted when the average wind speed is over 20 *m/s*. The video images were taken during strong winds at the Tokyo Bay Aqua Line. It shows that the flow around the vehicle on the bridge deck is greatly affected by the lane position. Therefore, in this study, the aerodynamic coefficients for the vehicle on the Tokyo Bay Aqua Line are obtained by computational fluid dynamic analysis, and next, the critical wind speed for the vehicle instability phenomenon is obtained from the vehicle stability

analysis under wind force calculated with the aerodynamic coefficients through CFD. Based on the above, the critical wind speed for instability phenomena is determined for each lane.

2. COMPUTATIONAL FLUID DYNAMIC

2.1. Numerical Setup

In present study, Large Eddy Simulation (LES) with Smagorinsky SGS model is conducted for flow around bridge deck-vehicle model. The Reynolds numbers chosen are Re=28,000. The study is implemented by StarCCM+. The computational domain is discretized using polyhedral mesh and prism meshes into total 13 million elements and, the first normal grid spacing located around wall unit y+<1. The simulation employs a constant velocity for the upstream boundary, a zero-gradient pressure for the outlet. Non-slip wall condition in bridge deck-vehicle model and periodic boundary condition in front and back are specified. The details of computational domain, dimensions of model and grid system near the model are shown in Fig. 1. Both velocity field and pressure field are iteratively calculated by AMG (Algebraic Multi-Gird) linear solver. The time progression used second order implicit. For the convection term, the bounded central differencing scheme was adopted. In this study, fluid numerical analysis is implemented on an empty medium truck with the Aqua bridge deck model. We focused on the aerodynamic coefficients of the vehicle at each lane on the bridge deck. The lane positions are defined as Lane1 to Lane4 in order from the windward side. In addition, the shape of the girder cross section including the railing and the median strip is modeled based on the drawing of the Aqua line. Models of bridge deck and the vehicle were validated respectively by comparing the analyzed value of the aerodynamic coefficients and the experimental values of previous studies(Sarwar, 2010 and Cheli, 2011).

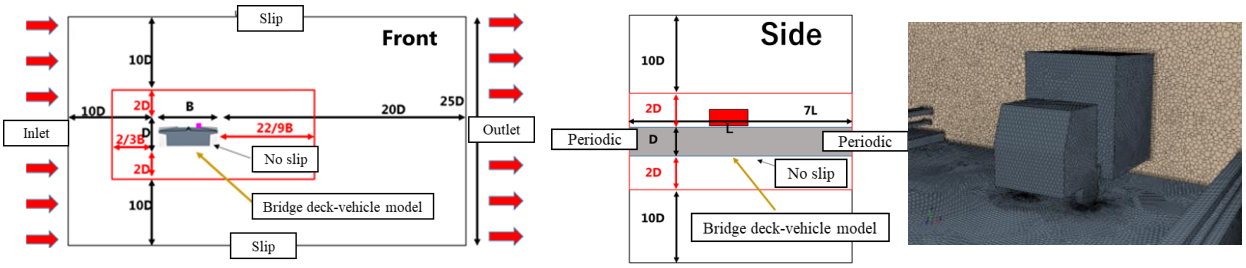

(a) Computational domain (front) (b) Computational domain (side) (c) grid system near the vehicle

Figure 1. Computational domain and grid system

2.2. CFD Results

The aerodynamic coefficients for the vehicle are defined as the following equations.

$$C_D = \frac{F_D}{\frac{1}{2}\rho U^2 A_f}, C_L = \frac{F_L}{\frac{1}{2}\rho U^2 A_S}, C_S = \frac{F_S}{\frac{1}{2}\rho U^2 A_S}, C_{MR} = \frac{M_R}{\frac{1}{2}\rho U^2 A_s h}, C_{MY} = \frac{M_Y}{\frac{1}{2}\rho U^2 A_s h}, C_{MP} = \frac{M_P}{\frac{1}{2}\rho U^2 A_S h} \quad (1)$$

The coefficient C_D, C_S, C_L, C_R, C_P, C_Y denote the coefficients of drag, side, lift, rolling, pitching, and yawing respectively. h is the distance between center of gravity of vehicle to the road surface. And, ρ is air density, U is wind velocity, A_S is area of vehicle side face and A_f is area of vehicle front face. The aerodynamic coefficients are compared for the lane position. Fig. 2 shows the flow field and Fig. 3 shows the time histories of the aerodynamic coefficients, C_S, C_{MR} and C_{MY} which have strong effects on vehicle instability. Fig. 3 shows that for all coefficients, the value of Lane1,

which is the leeward side, occupies the most disadvantageous value. On the other hand, the amplitude increases toward Lane4. This means that almost constant force acts on the vehicle in Lane1 while the force in other lanes on the leeward side causes the vehicle to become instable.

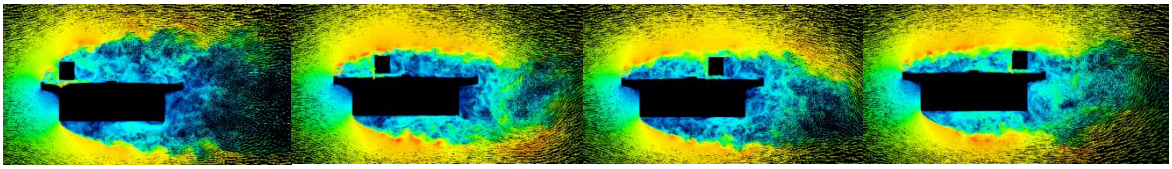

Figure 2. Instaneous flow field on lane 1, 2, 3 and 4

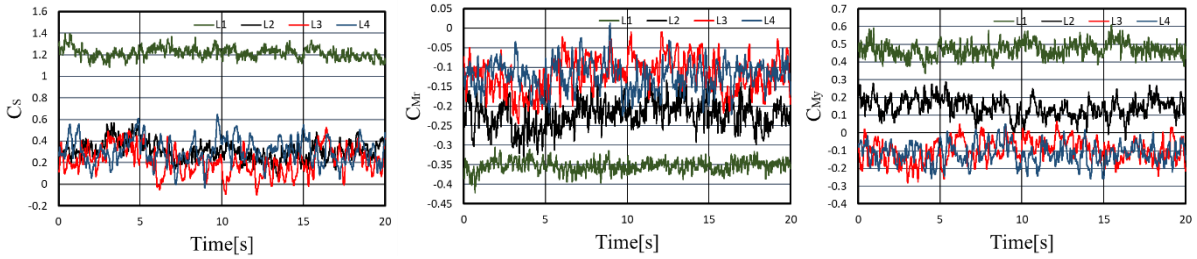

Figure 3. Aerodynamic coefficients, C_S, C_{MR} and C_{MY}

3. VEHICLE STABILITY ANALYSIS

3.1. Analysis method of vehicle motion

In the present study, a two-axle four-wheel non-articulated vehicle is employed. The vehicle dynamics is modelled as a combination of rigid body connected by several axle mass blocks with springs and damping devices (Fig.4). To evaluate stability of a vehicle subjected to wind, all acting forces in translational and rotational directions were considered. Based on the force equilibriums in three translational (x,y,z) and rotational (pitching, rolling and yawing), we can define normal forces on wheels considering also the driving condition and external forces including wind forces. Normal forces on the wheel can be defined as (note that the subscript ij on the normal force N_{ij} are as shown in Fig.4):

$$N_{11} = \frac{M_v L_2 (g-\ddot{Z}_v) - F_L L_2}{2(L_1+L_2)} + \frac{J_v \ddot{\phi} - M_R + hF_S}{4b} + \frac{I_v \ddot{\theta} - M_P - hF_D}{2(L_1+L_2)}, \quad N_{12} = \frac{M_v L_2 (g-\ddot{Z}_v) - F_L L_2}{2(L_1+L_2)} - \frac{J_v \ddot{\phi} - M_R + hF_S}{4b} + \frac{I_v \ddot{\theta} - M_P - hF_D}{2(L_1+L_2)}$$

$$N_{21} = \frac{M_v L_1 (g-\ddot{Z}_v) - F_L L_1}{2(L_1+L_2)} + \frac{J_v \ddot{\phi} - M_R + hF_S}{4b} - \frac{I_v \ddot{\theta} - M_P - hF_D}{2(L_1+L_2)}, \quad N_{22} = \frac{M_v L_1 (g-\ddot{Z}_v) - F_L L_1}{2(L_1+L_2)} - \frac{J_v \ddot{\phi} - M_R + hF_S}{4b} - \frac{I_v \ddot{\theta} - M_P - hF_D}{2(L_1+L_2)} \quad (2)$$

3.2. Instability condition

Accidents that occur when driving in an adverse condition are usually related to vehicle lateral instability due to rolling, sideslipping and rotation (Baker 1986). In this study, we evaluate two types of vehicle instability, namely, rollover and rotational instability as shown in Fig. 5. Rollover critical condition is when one of the wheels loses contact with the road surface. The time when a wheel is being lifted can be defined by looking at the condition when normal force described in Eq.4 becomes zero i.e., $N_{ij} = 0$. Next, rotation critical condition is when the front or rear part of the vehicle will rotate as shown in Fig.5b. The single axle slip is considered to occur when the

total lateral forces acting one axle, either the front of rear axle exceeds the critical resistance force for that axle, such that (here, μ_s is the side-slip friction coefficient)

Front axle slip:$(Fy_{11} + Fy_{12}) \geq \mu_s(N_{11} + N_{12})$ Rear axle slip:$(Fy_{21} + Fy_{22}) \geq \mu_s(N_{21} + N_{22})$ (3)

3.3 Vehicle stability Analysis results

Table 1 shows the critical wind speeds for rollover and rotation found from the vehicle stability analysis. The average wind speeds were obtained by dividing the critical wind speed obtained from Eqs. (4) and (5) by the gust coefficient. The gust coefficient was set to 1.3. From Table 1, the rotation limit wind speed was lower than the rollover limit wind speed in any lane.

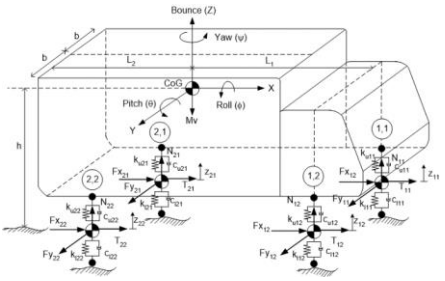

Figure 4. Vehicle dynamics rigid body model

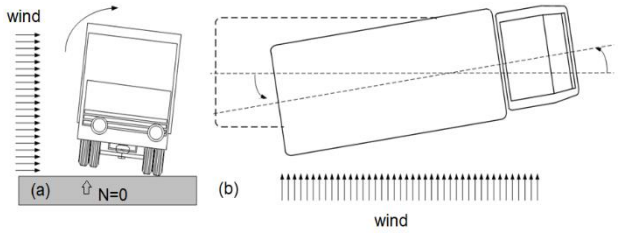

Figure 5. Instability condition (a) rollover (b) rotation

Table 1. Limit wind speed

Lane position	1	2	3	4
Limit wind speed of rotation[m/s]	18.4	23.7	26.9	26.1
Limit wind speed of rollover[m/s]	22	25.8	30.8	28.8

4. CONCLUSIONS

In this study, the flow field around the vehicle on the Tokyo Bay Aqua line was simulated by CFD, and the aerodynamic coefficients for the vehicle at each lane of bridge deck were investigated. In addition, a vehicle stability analysis was performed to describe the vehicle instability. Wind speed limit associated with each critical condition is determined. Results show the windward lane has the smallest wind speed limit and critical rotation occurs earlier than rollover in any lane.

ACKNOWLEDGEMENTS

This work was supported by JSPS KAKENHI Grant Number 20K04659 and NEXCO EAST Japan.

REFERENCES

Zhu, L.D., Li, L.D., Xu, Y.L. and Zhu, Q., 2012. Wind tunnel investigations of aerodynamic coefficients of road vehicles on bridge deck. Journal of Fluids and Structures, Vol.90, pp.35-50.

Wang, B., Xu, Y.L., Zhu,L.D., Cao, S.Y., and Li, Y.L., 2013. Determination of aerodynamic forces on stationary/moving vehicle-bridge deck system under crosswinds using computational fluid dynamics. Engineering Applications of Computational Fluid Mechanics, 7:3, 355-368.

Sarwar, M.W. and Ishihara, T., 2010. Numerical study on suppression of vortex-induced vibrations of box girder bridge section by aerodynamic countermeasures. Journal of Wind Engineering and Industrial Aerodynamics 98(12), 701-711.

Cheli, F., Corradi, R., Sabbioni, E. and Tomasini, G. 2011. Wind tunnel tests on heavy road vehicles: Cross wind induced loads—Part 1. Journal of Wind Engineering and Industrial Aerodynamics, Vol.99, pp.1000-1011.

Baker, C.J., 1986. A simplified analysis of various types of wind induced road vehicle accidents, J. Wind Eng. Ind. Aerodyn. 22(1), pp. 69–85.